

# A HIGH EFFICIENT DUAL-BOOST PHOTOVOLTAIC MICROINVERTER

ANITHA K.R

Dept. of Electrical and Electronics Engineering  
Dr. Ambedkar Institute of Technology

Dr. B.V SUMANGALA

Dept. of Electrical and Electronics Engineering  
Dr. Ambedkar Institute of Technology.

**Abstract**–This paper represents a high efficient micro inverter. Micro inverter performs the voltage elevation in two stages. The two stage configuration consists of two consecutive step-up converters. With this proposition it is possible to distribute the elevation effort to improve the overall efficiency of the photovoltaic microinverter. The proposed topology combines a traditional dc-dc boost converter in the first stage and dc-ac boost inverter in the second stage which consists of two step-up converters connected in the differential mode.

**Index Terms**– Microinverter, photovoltaic module, step-up converter.

## I. INTRODUCTION

Microinverters have gained increased attention for small-scale applications such as roof-top PV systems. The main advantage of this configuration is that the maximum power point tracking is distributed and decoupled for each PV module; reducing the impact of partial shading (clouds, surrounding buildings, snow, etc.) and module mismatch (aging) [1].

For the proper connection of grid a single photovoltaic module requires to boost its voltage around 20% above the grid peak voltage. Photovoltaic module requires an inverter to transform the direct current from solar cells to alternating current [2]. A conventional microinverter configuration consists of two stages of power converters: a dc-dc stage boost converter used to boost the voltage of dc-link above the peak grid voltage followed by a step down inverter connected to the grid. In general a high frequency transformer is used in the dc-dc stage to boost the voltage. For example a high switching frequency interleaved fly-back converter followed by a H bridge inverter is used [3]. As there are two stages of converter used one of them is having high frequency isolation transformer which causes less efficiency when compared to string inverter [4].

More recently, a single stage dc-ac step up topology has been proposed [5]-[9], which consists of two boost circuits connected in parallel based on differential output. The purpose of this inverter is to fulfil two functions being a single stage converter: increase the voltage of photovoltaic module and at the same time conversion from dc to ac. The drawback of this inverter is complexity in control [10]-[11]. This topology has less stage of conversion ratio and the losses are more. Hence the efficiency attained by

this inverter is low compared to the conventional two stage inverter [12].

In this paper, a dual-stage photovoltaic microinverter consisting of two successive step-up voltage converters; dc-dc and dc-ac execute voltage elevation. With this configuration, it is feasible to distribute the voltage step-up ratio effort between the two phases, improving overall efficiency.

## II. PROPOSED TOPOLOGY

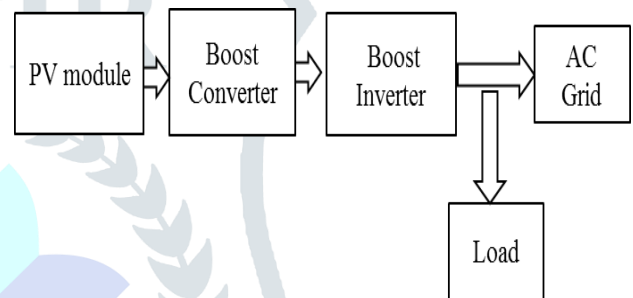


Fig.1: Proposed configuration consisting of the boost dc-dc stage and the boost dc-ac stage.

The proposed configuration of dual boost photovoltaic micro-inverter is shown in the fig 1. Here, PV module is used for the conversion of sun light into electricity by means of semiconducting materials exhibiting the photovoltaic effect. A boost converter is a DC-DC power converter which is used due to its easy design and no need for HF (high frequency) isolation. The boost inverter is used to convert dc-ac. It is the combination of two buck boost converters connected in differential mode. The fact that the first stage step-up ratio can be built at approximately 50 % of the conventional operations causes significant decrease in losses due to switching. This needs the dc-ac stage to execute voltage elevation as well, hence the use of the dual boost inverter.

### A. BOOST CONVERTER

Fig 2 shows the boost converter that raises the voltage of DC input to a given voltage of DC output. The source of input voltage is connected to an inductor. The source connected to the solid-state device works as a switch. A diode is the second switch used. The diode is connected to a capacitor which is in parallel to the load as shown in the figure.

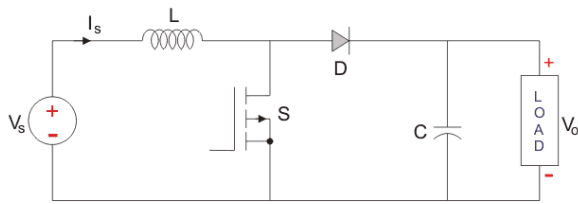


Fig 2: Boost converter

There are two working stages in the Boost converter.

Stage1: Switch is ON, Diode is OFF

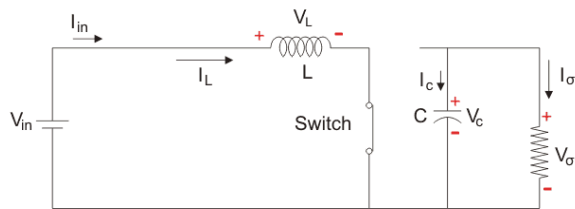


Fig 2(a): Boost converter when the switch is ON

When the switch is ON the diode becomes reverse biased and the current will flow through inductor, switch and then back to the source.

Boost converter during steady state operation, for stage 1 operation using KVL.

$$V_L = V_{in}$$

$$\therefore V_L = V_{in} = L \frac{dI_L}{dt}$$

$$\frac{\Delta I_L}{\Delta t} = \frac{\Delta I_L}{DT} = \frac{V_{in}}{L}$$

$$\text{Switch closed for } (\Delta I_L) = \frac{V_s DT}{L}$$

Stage 2: Switch is OFF, Diode is ON

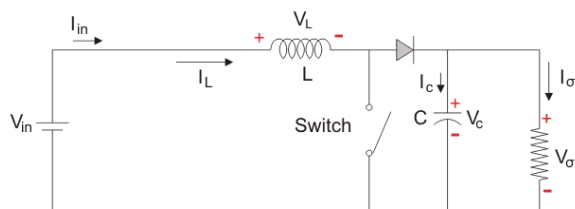


Fig 2(b): Boost converter when the switch is OFF

When the switch is OFF, the diode becomes forward biased to provide path for inductor current. The energy stored in the inductor will dissipate to the load resistance.

Boost converter during steady state operation, for stage 2 operation using KVL.

$$V_L = V_s - V_o = L \frac{dI_L}{dt}$$

$$\therefore \frac{dI_L}{dt} = \frac{V_s - V_o}{L}$$

$$\frac{\Delta I_L}{\Delta t} = \frac{\Delta I_L}{(1 - D)T} = \frac{V_s - V_o}{L}$$

$$\text{Switch open for } (\Delta I_L) = \frac{(V_s - V_o)(1 - D)T}{L}$$

The net change in inductor current,

$$\therefore (\Delta I_L)_{\text{closed}} + (\Delta I_L)_{\text{open}} = 0$$

$$\frac{V_s DT}{L} + \frac{(V_s - V_o)(1 - D)T}{L} = 0$$

$$\text{Solving for } V_o = \frac{V_s}{1 - D}$$

Here, D represents duty cycle in the range of 0 to 1.

### B. DUAL BOOST INVERTER

This is the combination of two buck boost converters and function one by one; in the positive portion of output voltage one converter will function whereas in the negative portion of output voltage another converter will function. It means at a time only two switches will operate at high frequencies at any given time and the switching strategy for the proposed inverter is as shown in the fig 4. As a consequence, there is a significant reduction in both switching and conduction losses. Here, C<sub>1</sub> and C<sub>2</sub> are the capacitors and their voltages are V<sub>1</sub> and V<sub>2</sub> respectively. d<sub>1</sub> and d<sub>2</sub> are instant duty ratios of the switches S<sub>1</sub> and S<sub>3</sub> respectively. The input and output voltages are represented by V<sub>in</sub> and V<sub>out</sub> respectively.

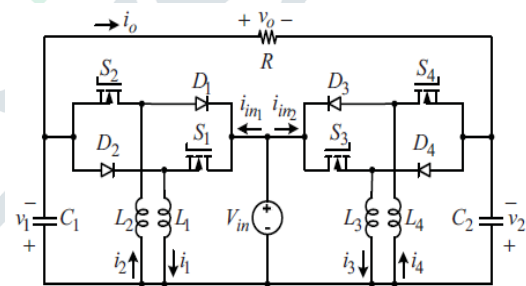


Fig 3: Differential dual buck boost inverter (DDBBI)

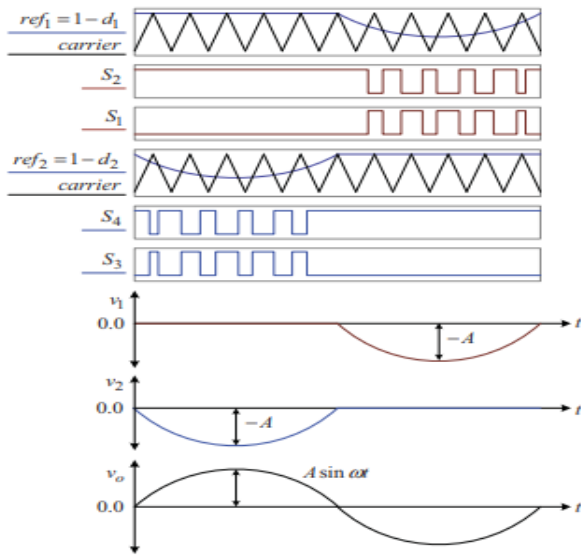


Fig 4: Switching strategy for the proposed inverter

During the positive half cycle of the sinusoidal output voltage, the switch S1 is in OFF condition and the switch S2 is in ON condition. At this time the capacitors C1 and C2 voltages are.

$$V_1 = \frac{-V_{in}d_1}{1 - d_1} = 0$$

$$V_2 = \frac{-V_{in}d_2}{1 - d_2} = A \sin(\omega t - \pi)$$

During the negative half cycle of the sinusoidal output voltage, the switch S3 is in OFF condition and the switch S4 is in ON condition. At this time the capacitors C1 and C2 voltages are.

$$V_1 = \frac{-V_{in}d_1}{1 - d_1} = A \sin \omega t$$

$$V_2 = \frac{-V_{in}d_2}{1 - d_2} = 0$$

From the above equations the duty ratios can be calculated as

For the positive half cycle,

$$d_1 = 0$$

$$d_2 = \frac{A \sin(\omega t - \pi)}{A \sin(\omega t - \pi) - V_{in}}$$

For the negative half cycle,

$$d_1 = \frac{A \sin \omega t}{A \sin \omega t - V_{in}}$$

$$d_2 = 0$$

OPERATION MODES OF DIFFERENTIAL DUAL BUCK BOOST INVERTER (DDBBI)

There are 8 modes of operations as shown in fig 5. Mode 1 to mode 4 operates for positive half cycle and mode 5 to mode 8 operates for negative half cycle.

Mode 1: During this stage, the switches S2 and S3 are ON while the switches S1 and S4 are OFF. Capacitor C2 will discharge current to the load through S2 and D2. The voltage across the inductor L3 is equal to the input voltage.

Mode 2 & 4: During this stage, the switch S2 is ON while the switches S1, S3 and S4 are OFF. Capacitor C2 will discharge current to the load through S2 and D2.

Mode 3: During this stage, the switches S2 and S4 are ON while the switches S1 and S3 are OFF. Capacitor C2 will discharge current to the load through S2 and D2.

Mode 5: During this stage, the switches S2 and S3 are OFF while the switches S1 and S4 are ON. Capacitor C1 will discharge current to the load through S4 and D4. The voltage across the inductor L1 is equal to the input voltage.

Mode 6 & 8: During this stage, the switch S4 is ON while the switches S1, S2 and S3 are OFF. Capacitor C1 will discharge current to the load through S4 and D4

Mode 7: During this stage, the switches S1 and S3 are OFF while the switches S2 and S4 are ON. Capacitor C1 will discharge current to the load through S4 and D4.

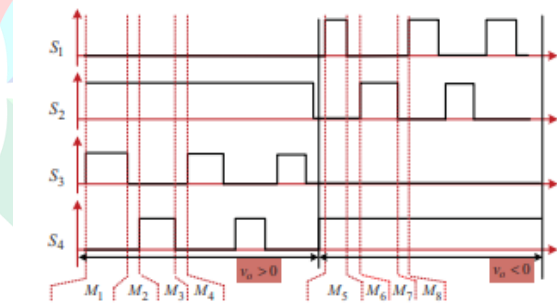


Fig 5: waveform of different operation modes

III. CONTROL SYSTEMS

A: Boost converter control

The boost converter, which consists of two cascaded control loops, is using a classic control system as shown in Fig. 6. A classical incremental conductance IC MPPT algorithm is used to obtain the voltage reference of the exterior control loops. Using a PI controller, the PV voltage error is controlled. The inductor current is also controlled by an inner PI control loop, and the switching signal S is acquired by means of a PWM.

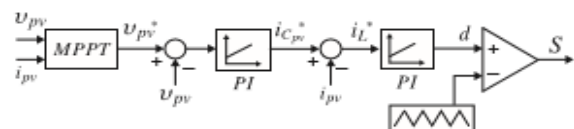


Fig 6: Control system of the dc-dc stage of proposed configuration.

B: Dual buck boost inverter control

Due to the system's high non-linearity, controlling the dual boost inverter is a difficult job, making linearization a complex process [11]. An easy control based on the hypothesis of differential flatness is used in this section. In theory, the variables of states and inputs can be depicted through the parts of flat output [15]. All variables can therefore be governed indirectly and there is no need for the linearization method. The overall system of control is shown in Fig. 7. It consists of three phases, where each dc-dc converter's control targets are dc-link voltage, active and reactive power, and output voltage.

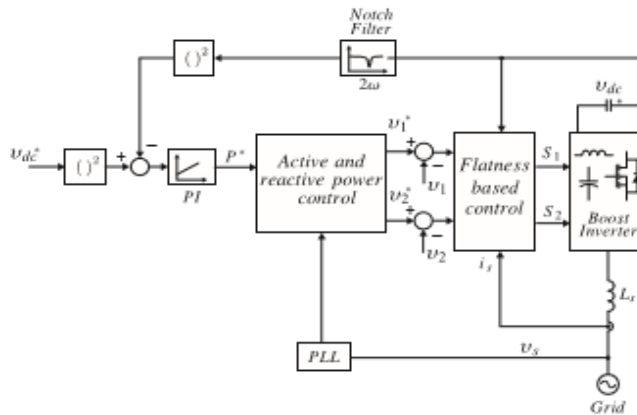


Fig 7: Control system of the dc-ac stage of proposed configuration.

IV. SIMULATION RESULTS

The system consisting of the boost converter and the dual boost inverter was simulated to validate the proposed configuration. The results of the each stage are shown following:

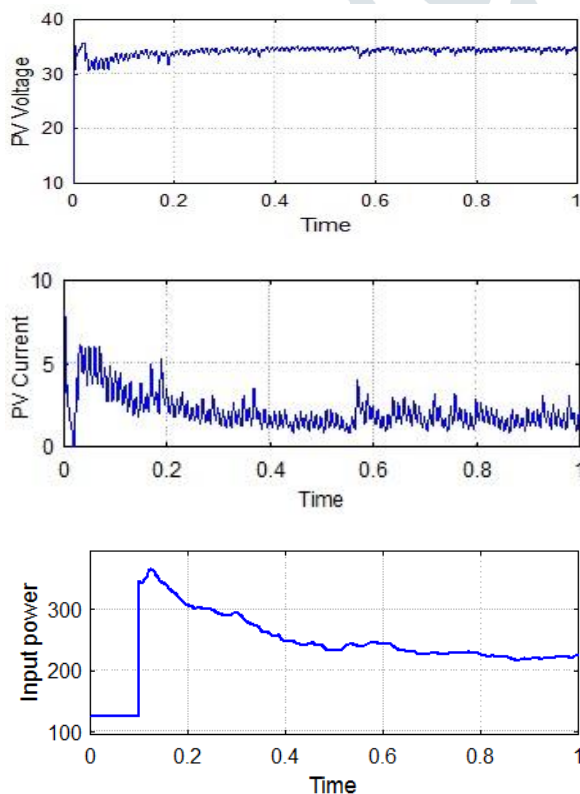


Fig 8: PV side results of the dual-stage boost micro-inverter: a) PV Voltage, b) PV current, c) PV power

Fig 8 shows the behaviour of PV. Whenever there is a change of solar irradiation occurs, the PV current and power will decrease. Fig 9 shows the behaviour of dc-dc boost converter voltage when its reference is 60V.

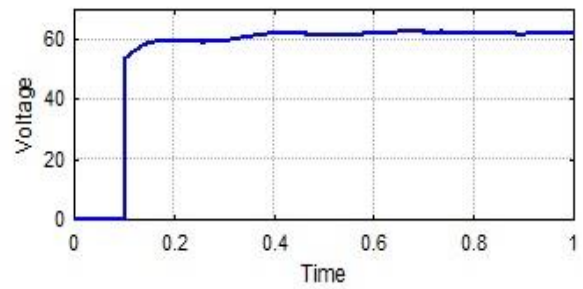


Fig 9: DC-DC boost voltage of dual boost micro-inverter

The results of dc-ac stage are shown in the fig 10. The output voltage of each boost converter can be observed in fig. 9.a. The signals of these figures are composed of dc and ac component. The dc component is 110V because the input voltage of the dc-ac stage is 60V.

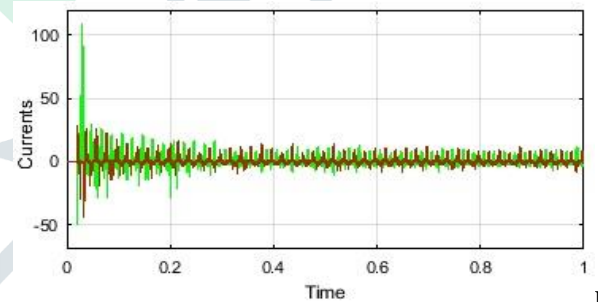
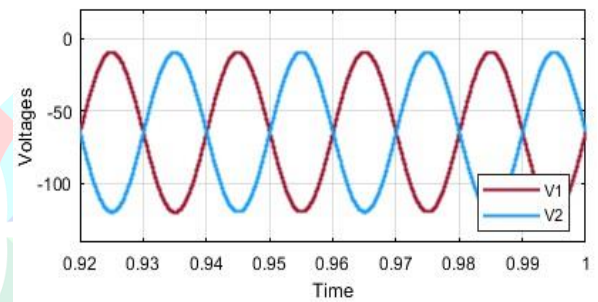
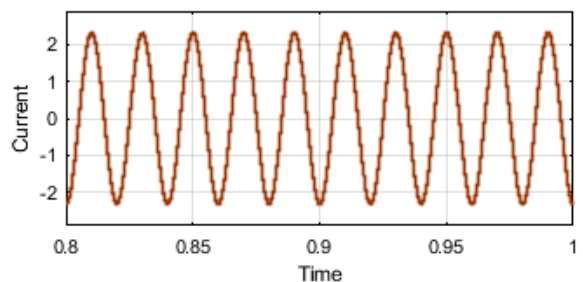


Fig 10: Results of the dual stage boost dc-ac converter: a) Capacitor voltages, b) Inductor currents.



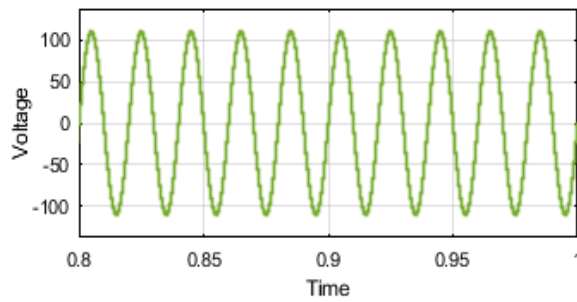


Fig 11: grid current and grid voltage of dual boost micro-inverter.

On the grid side, the waveform of the output current is closed to sinusoidal and in phase with the grid voltage, as shown in fig. 11.

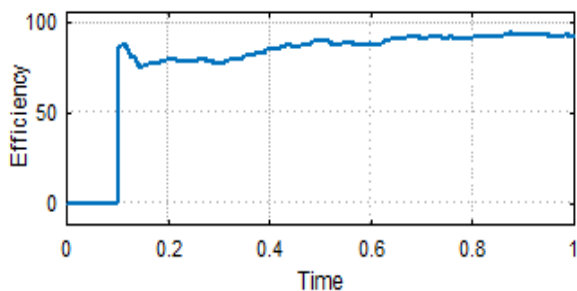


Fig 12: efficiency of the dual boost micro-inverter.

Fig. 12 shows the efficiency of dual boost micro-inverter, when the dc link voltage is 60V and ac output voltage is 110V.

## V. CONCLUSION

In this paper a dual boost PV micro inverter has been proposed. The proposed topology consists of an input dc-dc boost converter followed by a differential dual buck boost inverter. Simulation results show the effectiveness of the proposed micro-inverter configuration in increasing the efficiency. Simulation results shown that compared with the existing topology, the proposed topology allows an improvement in the efficiency by about 12 % and reduction in the THD of 11.81% to 0.76%.

## REFERENCES

- [1] S. Kouro, H. Abu-Rub, and F. Blaabjerg, *Power Electronics for Renewable Energy Systems, Transportation, and Industrial Applications Chapter 7: Photovoltaic Energy Conversion Systems*, 1st ed. John Wiley & Sons, 2014.
- [2] M. Fornage, "Method and apparatus for converting direct current to alternating current," Sep. 14 2010, uS Patent 7,796,412.
- [3] Y. Luo, "Alternating parallel fly back converter with alternated masterslave branch circuits," Jun. 29 2011, uS Patent App. 13/807,053.
- [4] S. Kouro, J. I. Leon, D. Vinnikov, and L. G. Franquelo, "Grid-connected photovoltaic systems: An overview of recent research and emerging pv converter technology," *IEEE Industrial Electronics Magazine*, vol. 9, no. 1, pp. 47–61, March 2015.
- [5] T. Konjedic, M. Truntic, M. Rodic, and M. Milanovic, "A singlestage boost dc-ac converter for single-phase grid-connected

photovoltaic systems," *Power Electronics South America*, Sept 2012.

[6] Y. Fang and X. Ma, "A novel pv microinverter with coupled inductors and double-boost topology," *IEEE Transactions on Power Electronics*, vol. 25, no. 12, pp. 3139–3147, Dec 2010.

[7] M. Coppola, P. Guerriero, F. D. Napoli, S. Daliento, D. Lauria, and A. D. Pizzo, "A pv ac-module based on coupled-inductors boost dc/ac converter," in *Power Electronics, Electrical Drives, Automation and Motion (SPEEDAM), 2014 International Symposium on*, June 2014, pp. 1015–1020.

[8] S. B. Kjær and F. Blaabjerg, "A novel single-stage inverter for the ac-module with reduced low-frequency ripple penetration," *Proceed. of Epe'2003*, Toulouse, France, 2-4 September, 2003.

[9] Y. Liu, M. Huang, J. Sun, and X. Zha, "Active power decoupling method for isolated micro-inverters," in *2014 International Power Electronics and Application Conference and Exposition*, Nov 2014, pp. 1222–1225.

[10] W. Zhao, D. D. C. Lu, and V. G. Agelidis, "Current control of gridconnectedboostinverterwithzerosteady-stateerror," *IEEE Transactions on Power Electronics*, vol. 26, no. 10, pp. 2825–2834, Oct 2011.

[11] D. Lopez, F. Flores-Bahamonde, S. Kouro, M. A. Perez, A. Llor, and L. Martinez-Salamero, "Predictive control of a single-stage boost dc-ac photovoltaic microinverter," in *IECON 2016 - 42nd Annual Conference of the IEEE Industrial Electronics Society*, Oct 2016, pp. 6746–6751.

[12] M. Jang, M. Ciobotaru, and V. G. Agelidis, "A single-phase gridconnected fuel cell system based on a boost-inverter," *IEEE Transactions on Power Electronics*, vol. 28, no. 1, pp. 279–288, Jan 2013.

[13] D. B. W. Abeywardana, B. Hredzak, and V. G. Agelidis, "A rule-based controller to mitigate dc-side second-order harmonic current in a singlephase boost inverter," *IEEE Transactions on Power Electronics*, vol. 31, no. 2, pp. 1665–1679, Feb 2016.

[14] R. O. Caceres and I. Barbi, "A boost dc-ac converter: analysis, design, and experimentation," *IEEE Transactions on Power Electronics*, vol. 14, no. 1, pp. 134–141, Jan 1999.

[15] M. Fliess, J. L'evine, P. Martin, and P. Rouchon, "Flatness and defect of non-linear systems: introductory theory and examples," *International journal of control*, vol. 61, no. 6, pp. 1327–1361, 1995.

[16] A. Gensior, O. Woywode, J. Rudolph, and H. Guldner, "On differential flatness, trajectory planning, observers, and stabilization for dc-dc converters," *IEEE Transactions on Circuits and Systems I: Regular Papers*, vol. 53, no. 9, pp. 2000–201